Suppression of staging in lithium-intercalated carbon by disorder in the host

J. R. Dahn
Moli Energy (1990) Limited, 3958 Myrtle Street, Burnaby, British Columbia, Canada V5C 4G2
and Department of Physics, Simon Fraser University, Burnaby, British Columbia, Canada V5A 1S6

Rosamaria Fong
Moli Energy (1990) Limited, 3958 Myrtle Street, Burnaby, British Columbia, Canada V5C 4G2

M. J. Spoon
Conoco Inc., P.O. Box 1267, Ponca City, Oklahoma 74603
(Received 30 May 1990)

We report electrochemical and x-ray-diffraction studies of the intercalation of lithium in graphite and in disordered carbons. The phase diagram of electrochemically intercalated graphite agrees well with previous work on samples prepared by chemical methods. The well-known staged phases present in intercalated graphite are absent in intercalated petroleum coke. Furthermore, the voltage $V(x)$ of Li/Li_xC_6 cells differs greatly when graphite or coke is used as the host. By heating coke to successively higher temperatures, we are able to increase the graphitization or crystalline order of the host in a continuous fashion and study the effect of this variation on the phase diagram of Li_xC_6 and on $V(x)$. We find that staged phases are suppressed at room temperature for hosts less ordered than a "critical disorder." A lattice-gas model with random site energies is used to model the effects of host disorder and qualitatively explains the suppression of staged phases and the changes in $V(x)$ with increasing disorder in the host. For a rectangular "density of sites," staged phases are suppressed when the width of the site energy distribution is greater than the magnitude of the mean-field attractive Li-Li interaction, which causes island growth and staging in intercalated graphite.

INTRODUCTION

The intercalation of lithium into graphite by vapor transport was first discovered by Herold in 1955.[1] Since then there have been many studies of Li_xC_6, where $0<x<1$ (Refs. 2–4) to identify staged phases. More recently the physics of staging in graphite intercalation compounds has been studied theoretically and experimentally.[5–10] The theoretical studies show that the driving force for the formation of staged phases is the strain-mediated attractive interaction between intercalant atoms within the same gallery.[9,11,12] The experimental studies of staging have focused on structural analysis of the staged phases,[13] and the determination of the phase diagram of the staged phases.[14,15]

Geurard and Herold[16] studied the intercalation of Li in graphite and in other carbons, including petroleum coke. They found that petroleum coke did intercalate Li but only up to $x=0.5$ in Li_xC_6. They did not report the existence of any staged phases in intercalated coke. Petroleum cokes are made up of graphite layers which are stacked "turbostratically" with random translations and rotations between adjacent layers.[17,18] As petroleum coke is heated to successively higher temperatures, the crystallinity of the material improves in a continuous manner[18] until finally, at heating temperatures near 3000 °C, crystalline graphite is made. In fact, premium petroleum cokes (e.g., XP coke from Conoco Inc.) are used as the starting material in the production of synthetic graphite.

Li atoms in intercalated graphite all occupy sites with the same nearest-neighbor environment between graphite layers which have $AAA\cdots$ stacking.[13] Thus, we expect the site energy, or binding energy of a Li atom to a site, to be site independent. As a consequence of the configurational disorder in petroleum coke, we expect the site energy to vary from site to site. Clearly, if the site energy variation is large enough, Li atoms will reside in the sites of lowest energy which are spatially separated and will not cluster together on adjacent sites within a single gallery as they would in the absence of a site energy variation. Therefore, we expect disorder in the host to suppress the formation of staged phases.

The effect of host disorder on phase separation in metal hydrides has been studied experimentally and theoretically.[19,20] Griessen found that the phase separation between phases of high and low H concentrations in crystalline hydrides was absent if amorphous-metal hosts were used instead. Instead, the H atoms remained uniformly distributed throughout the metal, and the material remained a single phase as the H concentration varied. Griessen used a lattice-gas model with random site energies to model the configurational disorder in the amorphous metal host. He showed that for a rectangular density of sites, phase separation was suppressed at a fixed temperature when the disorder exceeds a "critical disorder" at

which point the width of the site energy distribution equals the magnitude of the mean-field attractive interaction between intercalated H atoms. This interaction is mediated by the elastic strains caused by the lattice expansion which accompanies H intercalation. Using metal hydride hosts, it has not been possible to vary the host disorder in a continuous manner; only crystalline and amorphous hosts have been available.

Here we examine the intercalation of Li in petroleum coke, in a series of coke samples heated to successively higher temperature and in synthetic graphite. We use electrochemical cells to intercalate Li into the carbon samples and use the voltage of these cells to measure the chemical potential of the intercalated Li.[21] There have been previous attempts to intercalate Li into graphite electrochemically[22–24] but these have been plagued with side reactions (caused by electrolyte decomposition) and therefore are not reliable measurements of the chemical potential variation. Recently, we have learned how to overcome these experimental difficulties[25] and can now reliably and accurately intercalate Li into carbons using eletrochemical techniques. First, we discuss our experimental techniques, then begin by measuring the phase diagram of Li intercalated graphite at room temperature. Our data agree well with those measured on samples prepared using chemical methods and give us confidence in our methods. Then we report the structural changes in intercalated coke and the variation of the voltage with composition, $V(x)$, of Li/Li_xC_6 cells with coke electrodes. Next, we describe the results of our experiments on the heated coke samples and show that there is a transition between materials that show staged phases at room temperature and those that do not. Finally, we apply the theory developed by Griessen to qualitatively explain (1) the increase in the maximum amount of Li which can be intercalated from $x=\frac{1}{2}$ in coke to $x=1$ in graphite; (2) the flattening of $V(x)$ as the sample crystallinity improves; and (3) the sudden appearance of staging as the crystallinity of the host increases.

EXPERIMENTAL

Crystalline synthetic graphite powder was obtained from Lonza Corporation. We used two samples which differed only in their particle size distribution; KS-15 and KS-44 with mean particle sizes of 15 and 44 μm, respectively. We obtained identical results for the two samples. The lattice constants of these materials agree well with literature values for pure graphite[26] as shown in Table I.

Top premium petroleum needle coke designated XP was obtained from Conoco Inc. in the form of lumps about 1 cm^3. This material is about 99.5 wt. % carbon with sulfur (0.3 wt. %) as the major impurity. The spacing between carbon planes, $d(002)=3.46$ Å is typical for needle cokes. This coke is heat treated to approximately 1300 °C during the manufacturing process.

Petroleum coke samples were heated in an inert atmosphere to partially graphitize the coke. Some samples were heated in a Centorr furnace with a tungsten wire basket heating element at the University of British Columbia and others in a graphite resistance tube furnace at Conoco Inc. Infrared pyrometry was used for temperature measurement and control. The samples were raised to the treatment temperature and heated for 1 h. Table I lists the samples made. Figure 1 shows the variation of $d(002)$ with heating temperature. $d(002)$ was measured by

TABLE I. Carbon samples used in this work.

Sample	Heat treatment temperature (°C)	Furnace used	$d(002)$ (Å)
XP coke			3.460
1	1400	Graphite	3.458
2	1500	Graphite	3.450
3	1600	Graphite	3.439
4	1700	Graphite	3.438
5	1700	Centorr	3.435
6	1800	Graphite	3.434
7	1900	Graphite	3.432
8	1930	Centorr	3.430
9	2000	Centorr	3.424
10	2100	Graphite	3.409
11	2200	Graphite	3.398
12	2250	Graphite	3.393
13	2300	Graphite	3.383
14	2400	Graphite	3.378
15	2600	Graphite	3.366
16	2800	Graphite	3.363
17	3000	Graphite	3.355
Lonza graphite			3.355
Literature graphite (Ref. 26)			3.348

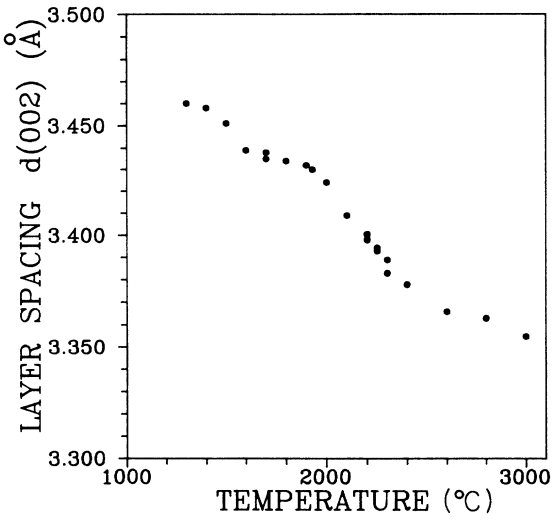

FIG. 1. Variation of layer spacing, $d(002)$, with heat-treatment temperature of Conoco XP coke.

least-squares refinement of the (002), (004), and (006) Bragg-peak positions. Our measurements have an error of ± 0.005 Å. Ruland[18] shows how the disorder in heated carbons smoothly correlates with the variation of $d(002)$.

The samples were then powdered by controlled grinding and sized using standard screens. Powders used for electrode fabrication were typically ground to -400 mesh (less than 38 μm).

Electrodes were prepared by mixing the carbon powder with binder solution followed by spreading on a copper collector. A "binder" solution of 4 wt.% EPDM (ethylene propylene diene monomer) in cyclohexane was prepared. Enough binder solution was added to the powder so that 2 wt.% EPDM remains in the electrode when the cyclohexane evaporates. Further pure cyclohexane was added to the stirred slurry until a syrupy viscosity was attained. Thin electrodes were then prepared by spreading the slurry on copper foil with a doctor blade spreader and allowing the cyclohexane to evaporate. The electrodes were then compressed between a set of rollers until the coating density was about 0.8 g/cm^3. Typical electrodes had a coating thickness of ~ 120 μm and a coating coverage of ~ 10 mg/cm^2. Our cells usually contain 1.2×1.2 cm^2 electrodes with an active mass near 14 mg. Typically, cycling currents are chosen to correspond to the intercalation of $\Delta x = 1$ in Li_xC_6 in a given time, say 50 h. We call this a 50-h rate. For the cathode described above, a 50-h rate corresponds to a current of 104 μA.

Two electrode electrochemical cells were constructed using these cathodes, Li foil (Lithium Corporation of America), porous polypropylene separators, and a non-aqueous electrolyte containing a dissolved Li salt. Throughout the course of this work we used two different salts and several different solvent combinations. Typical electrolytes used were 1 M $LiAsF_6$ dissolved in a 50:50 mixture of propylene carbonate (PC) and ethylene carbonate (EC), 1 M $LiAsF_6$ in EC/ethylmonoglyme (EIG) (50:50), 1 M $LiN(CF_3SO_2)_2$ in EC/ethylmonoglyme, and 1 M $LiN(CF_3SO_2)_2$ in EC/dimethoxyethane (DME) (50:50). The salts $LiAsF_6$ and $LiN(CF_3SO_2)_2$ were obtained from Lithium Corporation of America and 3M Corporation, respectively. The latter salt was dried under vacuum at 140 °C prior to use. The solvents PC, EC (Texaco), and ethylmonoglyme (Ferro Corporation) were all distilled prior to use. Dimethoxyethane from Aldrich was used as received. All electrolytes were tested for moisture and were not used if the moisture content was greater than 100 ppm.

In this work, we observed no difference in the *reversible* cycling of Li/carbon cells as a function of electrolyte type. The irreversible capacity which is observed on the first discharge of Li/carbon cells,[25] however, does differ between these electrolytes. As described in Ref. 25, simple electrolytes containing PC as the sole solvent do not work well in Li/graphite cells because Li ions solvated by PC co-intercalate between the graphite layers. Apparently, the addition of EC to the electrolyte changes the solvation cloud about the Li ion enough to almost entirely suppress co-intercalation. Since EC is a solid at room temperature, EC containing electrolytes are normally based on multisolvent blends, such as those described above, for convenience. We have learned recently that additions of crown ethers to PC containing electrolytes also change the solvation cloud around the Li ion and apparently prevent co-intercalation.[28] Some results reported here are for cells with 1 M $LiN(CF_3SO_2)_2$, 1M 12-Crown-4/PC electrolyte. Solvent co-intercalation does not occur in petroleum coke when PC-based electrolytes are used.[25]

Two types of electrochemical cells were used here. First, we used the hermetically sealed test cells described in Ref. 25 to determine $V(x)$ of Li/Li_xC_6. Second, electrochemical cells with beryllium x-ray windows[27] were used so that structural changes in the intercalated carbons could be measured *in situ* as x in Li_xC_6 is changed by charging or discharging the cells. This technique has been used successfully to study the structural changes caused by the intercalation of Li in many hosts (e.g., Refs. 29 and 30). Our x-ray diffractometer uses Cu$K\alpha$ radiation.

To determine $V(x)$ and the differential capacity $-dx/dV$, cells were charged and discharged using constant currents between fixed voltage limits at 21 ± 1 °C. The cell cyclers maintain stable currents to $\pm 1\%$. Changes in x are calculated from the cathode mass, the constant current, and the time of current flow. Data are typically measured whenever V changes by ± 0.010 V.

RESULTS

Figure 2 shows the first cycles of a Li/graphite cell at a nominal 40-h rate. This cell used 1 M $LiN(CF_3SO_2)_2$, 1 M 12-Crown-4/PC electrolyte. The plateau near 0.7 V observed during the first discharge is caused by the reaction of Li atoms at the graphite surface with electrolyte to form a film of reaction products.[25] This ionically conducting and electronically insulating film prevents further reaction with electrolyte once its thickness increases to a value which prevents electron tunnelling. The crown-

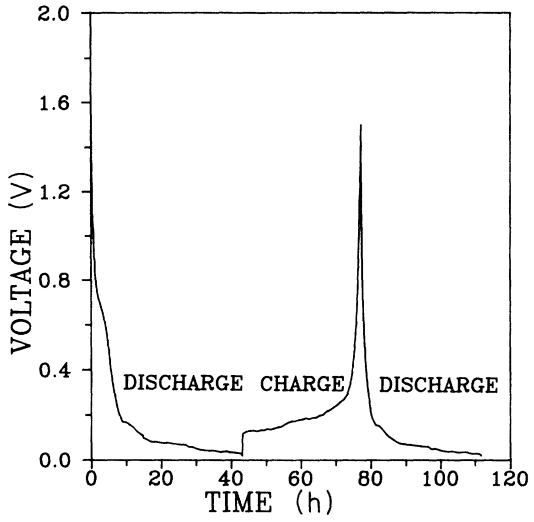

FIG. 2. The first cycles of Li/graphite cell. The currents used correspond to a change $\Delta x = 1$ in Li_xC_6 in 40 h.

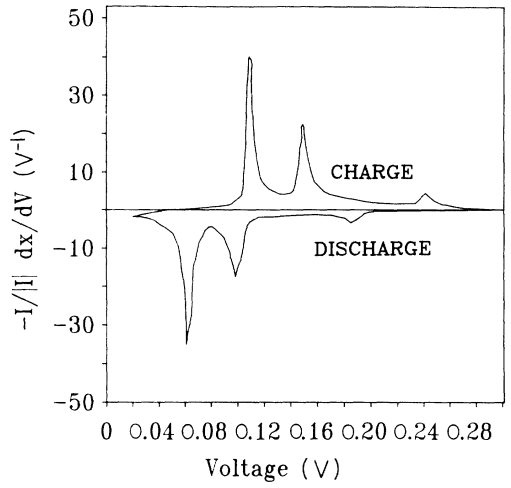

FIG. 4. $-dx/dV$ vs V for a Li/graphite cell cycled at an 80-h rate.

ether addition prevents co-intercalation of the solvent molecules into the graphite, minimizing the irreversible reactions evident above 0.5 V. The first discharge shows only a small amount of excess capacity compared to the second discharge.

The plateaus near 0.1 V correspond to the reversible intercalation of Li in graphite. Figure 3 shows $V(x)$ for the same Li/graphite cell measured during a later cycle at an 80-h rate. The plateaus in $V(x)$ are more easily identified when the derivative $-dx/dV$ is plotted versus V (Fig. 4). (The offset between charge and discharge is caused by the ir drop in the internal resistance of the cell.) Plateaus in $V(x)$ and peaks in $-dx/dV$ are normally found when the intercalation compound exists as a mixture of coexisting phases over some range of x.[21] There are many regions where phases of different stage index coexist in the Li-C phase diagram.[6,7,9,15] Our constant temperature intercalation of Li into graphite corresponds to a horizontal cut across the Li-graphite phase diagram at room temperature. According to the literature we expect to sequentially see coexistence of unintercalated graphite and stage 4, of stages 4 and 3, of 3 and a liquidlike stage 2 ($2L$), of $2L$ and 2, and of 2 and 1 as Li is intercalated into graphite at 300 °C. Our data show evidence for only three plateaus, not five, although we do not expect to be able to distinguish plateaus separated by less than 10 mV with the experiment described here. The plateau between $x = \frac{1}{2}$ and $x = 1$ (Fig. 3) corresponds to the coexistence of stages 1 and 2. The plateau between $x \approx 0.25$ and $x = \frac{1}{2}$ is thought to correspond to the stage 3–stage 2 coexistence; we see no evidence for the $2L$ phase. We have not identified the small plateau near $x = 0.1$.

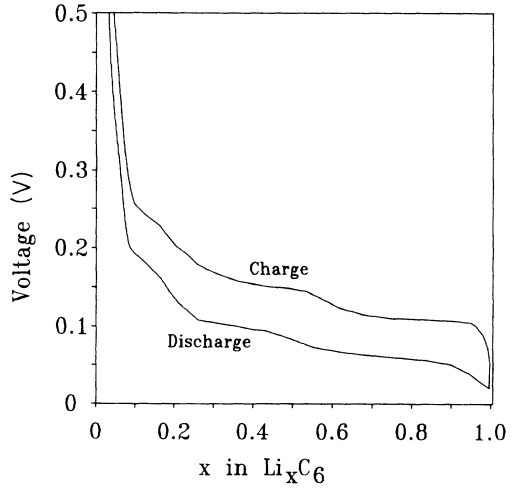

FIG. 3. $V(x)$ for a Li/graphite cell charged and discharged using a current corresponding to a change $\Delta x = 1$ in Li_xC_6 in 80 h.

Figure 5 shows portions of x-ray diffraction (XRD) profiles of the cathode of a Li/graphite *in situ* x-ray cell taken at different x in Li_xC_6 during the constant current charging of the cell at a 40-h rate. The average sample composition x for each profile is indicated in the figure caption. We have plotted the region of the profile corresponding to the graphite (002) Bragg peak, which indicates the average spacing between graphite planes. Scan 1 was taken when the cell was almost completely discharged, at $x = 0.9$. This scan shows that the sample is almost predominantly stage 1, since the predominant peak is at a scattering angle of 24.12° corresponding to the average layer spacing of LiC_6 (see Table II). As Li is removed from the sample, the stage-2 phase forms at the expense of stage 1 as a new Bragg peak near 25.30° grows. Next, stage 2 disappears while stage 3 and then unintercalated graphite appear. Figure 6 shows the amounts of the phases present during this constant current recharge measured by integrating the Bragg-peak intensity corresponding to each phase for each value of x.

We only measured the powder pattern in our x-ray experiment at 12 values of x during this charge. Therefore, we may not see narrow line phases like stage 4 in this experiment. This experiment was done to prove that the

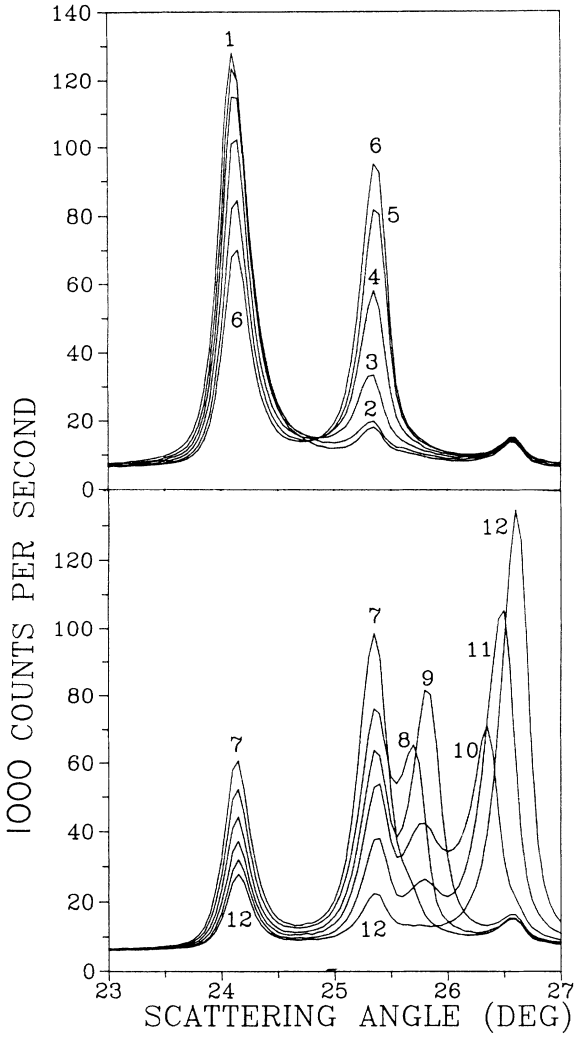

FIG. 5. *In situ* x-ray diffraction profiles in the (002) region measured during the constant current charging of a Li/graphite cell at a 40-h rate. The values of x in Li_xC_6 (measured from the cathode mass and the charge transferred) corresponding to the numbered scans in the figure are 0.90, 0.84, 0.72, 0.66, 0.59, 0.54, 0.48, 0.41, 0.35, 0.29, 0.23, and 0.17 for scans 1 to 12, respectively.

plateaus in Fig. 3 and the peaks in Fig. 4 correspond to the traversal of the phase diagram for Li_xC_6. A further experiment with very fine resolution in x and V will be done to look for evidence of the stage-4 and -2L phases. This is planned to be the subject of a future publication.

We can measure the chemical potential μ of intercalated Li with respect to the chemical potential of Li in Li metal from the data in Figs. 3 and 4. The cell voltage V is[21]

$$V = -\mu/e \ ,$$

where e is the magnitude of the electron charge. Theoretical models of staging can be tested if differences in μ for the stage n, $n+1$, etc. coexistence plateaus are known. Our measurements are given in Table III. We used the average of the plateau positions measured during charging and discharging because the ir drop shifts $V(x)$ in opposite directions when I changes sign.

Figure 7 shows $V(x)$ for the second discharge and charge of Li/coke and Li/(coke heated to 2100 °C) cells. These cells contained 1 M $LiN(CF_3SO_2)_2$/PC and 1 M $LiAsF_6$/PC/EC electrolytes, respectively. Other cells made using the other electrolytes discussed in the experimental section showed identical reversible cycling behavior. These data are quite different from that in Fig. 3 for Li/graphite cells. First, the maximum amount of Li that can be intercalated in coke and in coke heated to 2100 °C is $x = 0.5 \pm 0.03$ and 0.58 ± 0.06, respectively, much lower than $x = 1$ for graphite. The errors quoted above are from averages over several experiments. Second, Li intercalation in these disordered carbons begins near 1.0 V

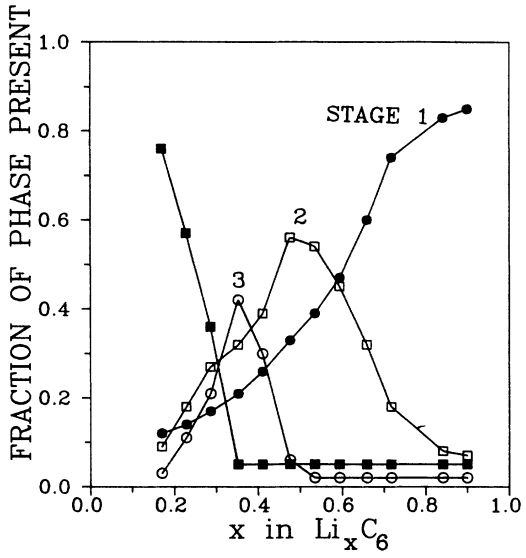

FIG. 6. Variations in the fractions of the phases stage 1, 2, 3, and unintercalated graphite present during the same constant current charge as for Fig. 5. ●, stage 1; □, stage 2; ○, stage 3; ■, graphite. More than two phases coexist at a time because the sample is not in equilibrium while the current flows.

TABLE II. Average graphite-layer spacing in Li_xC_6 as a function of x and stage index. Literature values are from Ref. 13.

x in Li_xC_6	d(002) Observed (Å)	d(002) Literature (Å)	Stage index
0	3.355	3.355	Graphite
~0.25	3.450	3.460	3
0.5	3.520	3.530	2
1.0	3.700	3.706	1

TABLE III. Chemical potential of Li in Li_xC_6 with respect to Li metal in two-phase coexistence regions at 21 °C.

Coexistence region	μ (eV)
Stage 1-2	-0.082 ± 0.005
Stage 2-3	-0.128 ± 0.005

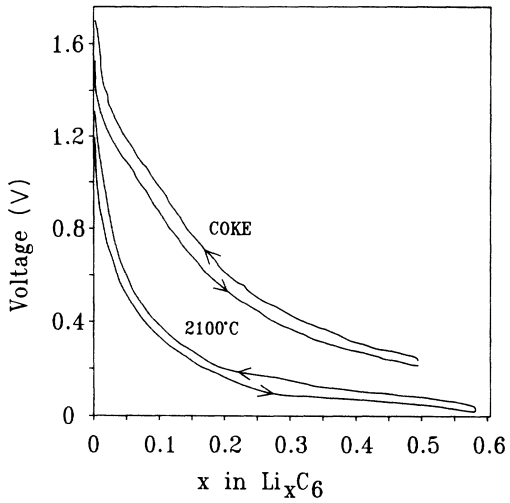

FIG. 7. $V(x)$ for the second cycle of Li/coke and Li/(coke heated to 2100 °C) cells. The data for the Li/coke cell have been offset by +0.2 V for clarity.

versus Li metal. Finally, the Li/coke cell shows no evidence of plateaus indicative of two-phase coexistence, while $V(x)$ for the Li/(coke heated to 2100 °C) cell flattens appreciably near $x=0.4$. *In situ* x-ray experiments were performed to learn if these materials are single-phase intercalation compounds.

A Li/petroleum coke *in situ* x-ray cell was prepared and was discharged and charged once at a rate of 40 h for $\Delta x=1$ in Li_xC_6. X-ray profiles taken of the freshly assembled cell and the cell after the first cycle were the same. The cell was then discharged at the same rate while acquiring 10-min XRD scans over the (002) region at 1.2-h intervals. The average x varies by only 0.004 during each scan. Figure 8 shows five of these scans at various x. The (002) peak shifts smoothly indicating a single phase, the layer spacing of which increases as Li is intercalated. The half-width ($\approx 1.7°$) of the (002) peak does not change significantly indicating that the crystalline disorder in petroleum coke is unaffected by Li intercalation.

A similar *in situ* x-ray experiment on a Li/(coke heated to 2100 °C) cell also showed single-phase intercalation. Figure 9 shows several (002) profiles taken at various x in Li_xC_6. Again, the (002) peak smoothly shifts as Li is intercalated and no change in peak width with x is observed.

Figure 10 shows the average spacing between carbon sheets in Li_xC_6 for coke, coke heated to 2100 °C, and graphite as a function of x. Discrete points have been plotted for the pure phases of Li intercalated graphite. The results of two separate experiments on the heated coke have been included. The lattice expansion with x in both coke and coke heated to 2100 °C is nonlinear although much more so in the latter case. Nonlinear lattice expansion is common in layered intercalation compounds.[31,32]

There is no evidence for the formation of staged phases in intercalated coke or in coke heated to 2100 °C. The best evidence we have that these materials are uniformly intercalated at all x is the absence of the two-phase coexistence regions which commonly border the pure staged phases. For these coke samples, no coexisting phases were detected by x-ray diffraction or by measurements of $V(x)$ and dx/dV. We return to the interpretations of $V(x)$ for coke heated to 2100 °C below.

It is clear that staged phases are eliminated if there is sufficient disorder in the graphite host. The effect of reducing the disorder in the host lattice was investigated by testing a series of Li/coke cells containing untreated coke

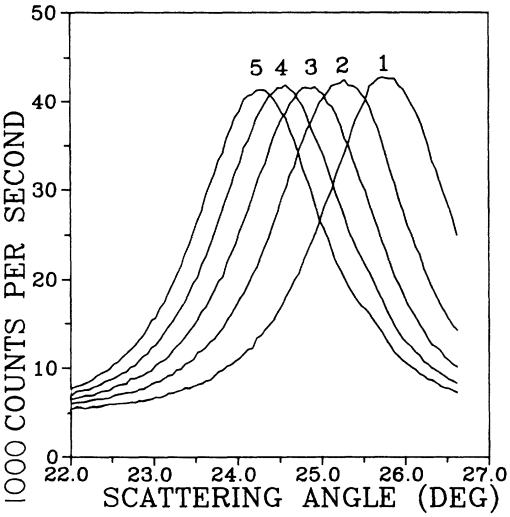

FIG. 8. *In situ* x-ray diffraction profiles in the (002) region measured during the constant current discharging of a Li/petroleum coke cell. The current used corresponds to a change $\Delta x=1$ in Li_xC_6 in 40 h. The values of x that correspond to the numbered scans are 0.005, 0.13, 0.25, 0.37, and 0.50, respectively, for scans 1 to 5.

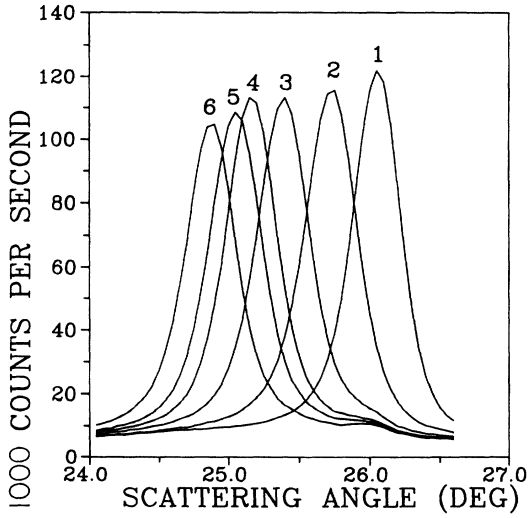

FIG. 9. *In situ* x-ray diffraction profiles in the (002) region measured during the constant current discharging of a Li/(coke heated to 2100 °C) cell. The currents used correspond to a change $\Delta x=1$ in Li_xC_6 in 40 h. The values of x that correspond to the numbered scans are 0.005, 0.10, 0.19, 0.28, 0.37, and 0.58, respectively, for scans 1 to 6.

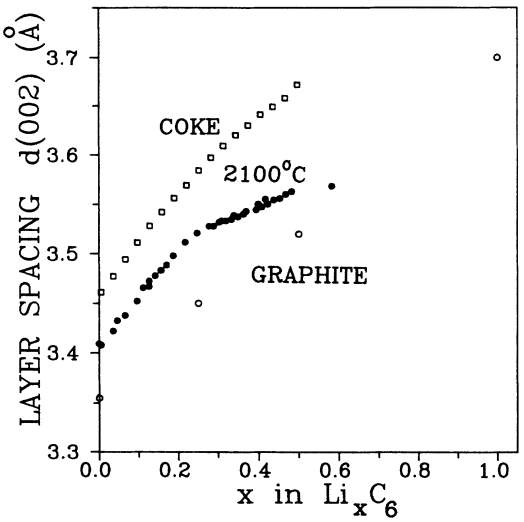

FIG. 10. Variation of the average layer spacing with x in Li_xC_6 measured using *in situ* x-ray diffraction for coke, □; coke heated to 2100 °C, ●; and graphite , ○. The graphite data are for the pure staged phases as described in the text.

and coke treated at 1930, 2100, 2200, and 2300 °C. Figure 11 shows $-dx/dV$ versus V on discharge for these cells. The behavior shown here is reversible. For coke heated to 1930 °C and for untreated coke, dx/dV is smooth and featureless, but for material treated at 2200 °C and 2300 °C two well-defined peaks appear. These match the features in dx/dV in Li/graphite cells (Fig. 4) which have been shown to correspond to the coexistence of different stage phases. We interpret this as evidence for staging in the 2200 °C and 2300 °C treated cokes, and the absence of staging in material treated at 1930 °C.

The material heated at 2100 °C shows intermediate behavior which is difficult to interpret although our *in situ* x-ray results suggest this corresponds to single-phase behavior. Further data on samples heated to between 1930 °C and 2200 °C would assist in this interpretation.

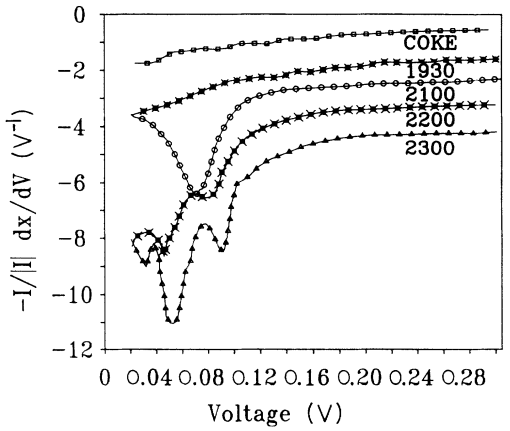

FIG. 11. $-dx/dV$ vs V for Li/treated coke cells measured using a current corresponding to a change $\Delta x = 1$ in 80 h. The treatment temperature of the coke used is indicated in the figure. The data have been offset for clarity: coke, no offset, 1930° C, -1 V^{-1}; 2100 °C, -2 V^{-1}; 2200 °C, -3 V^{-1}; 2300 °C, -4 V^{-1}.

DISCUSSION

There are systematic differences between the intercalation of Li in coke, heated cokes, and graphite which we will now explain. The differences are as follows.

(1) As coke is heat treated to higher temperatures, $V(x)$ flattens (Fig. 7) and eventually the dx/dV curve resembles that of graphite (Fig. 11).

(2) As coke is heat treated at successively higher temperatures, we begin to see evidence of staged phases above 2200 °C.

(3) The maximum amount of Li that can be intercalated into these graphitic carbons increases from $x = 0.5$ to $x = 1.0$ in Li_xC_6 as the carbon is made crystalline.

These trends can be qualitatively understood using a simple lattice-gas model of intercalation which accounts for the disorder in the coke samples.

Theoretical studies of staging have shown that the driving force for the formation of staged phases is the strain-mediated attractive interaction between intercalant atoms within the same gallery.[9,11,12] This interaction causes clustering of atoms into islands within a single gallery; other interactions then cause the islands to order into staged structures. For simplicity, we consider *only a single gallery* and the clustering of intercalant atoms within it. We assume that once clustering within the gallery occurs, staged phases will form in the bulk material. We can use a very simple model (which retains the essential physics) developed by Griessen[19] for amorphous metal hydrides to discuss the effect of configurational disorder on $V(x)$ and staging in intercalated coke.

Li atoms in intercalated graphite occupy sites with the same nearest-neighbor environment. We expect the site energy or binding energy of a Li atom to a site E to be site independent. In petroleum coke, because of the turbostratic disorder[18] we expect the site energy to vary from site to site. Like Griessen,[19] we define a density of sites function $n(E)$, which gives the probability of finding sites at energy E, such that

$$\int_{-\infty}^{\infty} n(E)dE = 1 , \tag{1}$$

which implies $x = 1$ in Li_xC_6 is the maximum. The average concentration x of Li in Li_xC_6 is given by

$$x = \int_{-\infty}^{\infty} n(e)\bar{x}(E,\mu,T,x)dE , \tag{2}$$

where $\bar{x}$ is the average occupation of all sites of energy E. We now assume that the strain-mediated attractive interaction is long range and therefore depends only on x and can be treated with mean-field theory. Then, since μ must be uniform everywhere,

$$\mu = kT \ln\left[\frac{\bar{x}}{1-\bar{x}}\right] + E + Ux . \tag{3}$$

Here U/N is the energy of interaction between any two Li atoms intercalated in the host, N is the number of

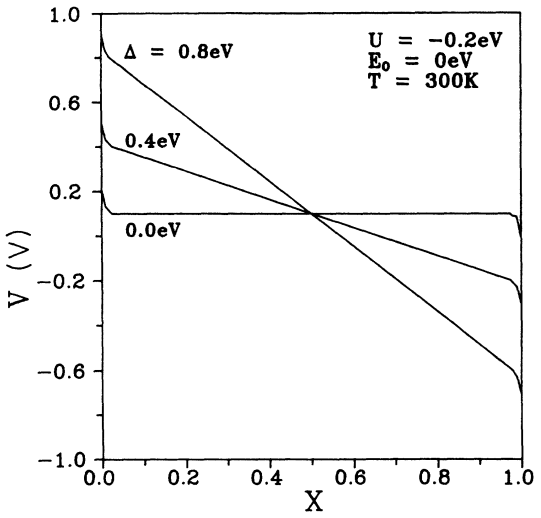

FIG. 12. Model calculation showing the effect of the width of the site energy distribution Δ on $V(x)$. The model parameters are described in the text.

available sites, and k is Boltzmann's constant. Solving (3) for $\bar{x}$ and inserting in (2), we obtain

$$x=\int_{-\infty}^{\infty} n(E)\frac{1}{(e^{(E+Ux-\mu)/kT}+1)}dE \ , \tag{4}$$

which corresponds to Eq. (13) in Ref. 19.

To qualitatively describe intercalated graphite, we set $n(E)=\delta(E_0)$ in (4). Then we can solve to get

$$\mu=E_0+Ux+kT\ln\left[\frac{x}{1-x}\right] . \tag{5}$$

For this variation of μ with x, phase separation into phases of high and low Li concentration occurs for $T<T_c=|U|/4k$ when U is negative.[33] For $T>T_c$, the Li randomly occupies the available sites. For Li intercalated graphite, staged phases predominantly disappear above 600 K (Ref. 15) so we set $U=-0.2$ eV. We then calculate $V=-\mu/e$ and adjust E_0 to $E_0=0$ to obtain qualitative agreement with Fig. 3. Our calculated $V(x)$ is given in Fig. 12 for $E_0=0$ eV.

To describe petroleum coke, we take a rectangular density of sites such that

$$n(E)=\tfrac{1}{2}\Delta \text{ for } E_0-\Delta\le E\le E_0+\Delta$$

and

$$n(E)=0 \text{ otherwise.}$$

Then, we solve for μ following Griessen and obtain

$$\mu=E_0+U(x)-\Delta+kT\ln\left[\frac{e^{(2\Delta/kT)}-1}{1-e^{2\Delta(x-1)/kT}}\right] . \tag{6}$$

For $\Delta\gg kT$, this reduces to $\mu=E_0-\Delta+(U+2\Delta)x$. We also find following Griessen that

$$\frac{T_c}{T_c(\Delta=0)}=\frac{-4\Delta/U}{\ln[(1-2\Delta/U)/(1+2\Delta/U)]} . \tag{7}$$

Figure 12 shows $V=-\mu/e$ for $E_0=0$ eV, $U=-0.2$ eV with $\Delta=0.8$ and 0.4 eV calculated using Eq. (6). As Δ increases, the slope of $V(x)$ increases and there is no longer any phase separation. Figure 3 in Ref. 19 shows $T_c/T_c(\Delta=0)$ plotted versus $2\Delta/|U|$. For $2\Delta/|U|>1$, there is no phase separation at any temperature. For $2\Delta/|U|<1$ phase separation occurs at successively higher temperatures as Δ decreases. Phase separation occurs only at $T=0$ at the "critical disorder" $2\Delta/|U|=1$.

The model shows that phase separation is suppressed if the width of site energy distribution (2Δ) is greater than the mean-field attractive interaction. When the site energy variation is large, Li atoms first occupy the sites of lowest energy, which are spatially separated, and do not form clusters as they would in the absence of a site energy variation. Figures 7 and 12 show that Δ for petroleum coke must be of order 1 eV; if we use $U=-0.2$ eV, then $2\Delta/|U|\approx 10\gg 1$, so we do not expect phase separation or staged phases in Li intercalated coke. Apparently, Li atoms in some sites in petroleum coke are much more tightly bound than in intercalated graphite. On the other hand, about half of the sites in petroleum coke have $E>0$ eV with respect to Li metal, which affects the maximum amount of Li that can be intercalated.

As coke samples are heat treated the disorder in the samples decreases so the width in the site energy distribution must also decrease. Figure 12 shows that $V(x)$ flattens as this occurs, and an increase in the maximum amount of Li that can be intercalated above 0 V is observed in qualitative agreement with Fig. 7. [For $V(x)\le 0$ V, Li will no longer intercalate into any host in equilibrium, but will simply electrodeposit as metal on the surface.] Finally, as crystalline order increases further, we eventually see evidence for phase separation and staged phase formation in our coke samples heat treated above 2200 °C. This is consistent with samples heat treated to near 2100 °C having $2\Delta/|U|\approx 1$.

The structure of disordered carbons has been extensively studied in the past.[18] Theoretical study of the expected site energy distribution based on the crystalline disorder is needed before a quantitative interpretation of our data is possible. If there is no phase separation, $n(E)$ can be obtained experimentally from $V(x)$ and compared to a theoretical calculation.

Further studies of samples heated to temperatures between 1900 °C and 2200 °C are needed to examine when the onset of staging begins. These studies could be extended to other alkali metals to see if a consistent model of the effects of lattice disorder can be formulated. Finally, we plan careful *in situ* x-ray diffraction experiments on Li intercalated graphite to examine the phase diagram at low x to determine if the stage-4 and the $2L$ phases are present at room temperature.

[1]A. Herold, Bull. Soc. Chim. France **187**, 999 (1955).
[2]R. Juza and V. Wehle, Nature **52**, 560 (1965).
[3]M. Bagouin, D. Guerard, and A. Herold, C. R. Acad. Sci. Ser. C **262**, 557 (1966).
[4]D. Guerard and A. Herold, C. R. Acad. Sci. Ser. C **275**, 571 (1972).
[5]P. Delhaes and J. P. Manceau, Synth. Met. **2**, 277 (1980).
[6]J. E. Fischer, C. D. Fuerst, and K. C. Woo, Synth. Met. **7**, 17 (1983).
[7]J. E. Fischer and H. J. Kim, Synth. Met. **12**, 137 (1985).
[8]S. Rabii, G. Loupias, J. Chomilier, and D. Guerard, Synth. Met. **23**, 175 (1988).
[9]G. Kirczenow, Can. J. Phys. **66**, 39 (1988).
[10]G. Kirczenow, Synth. Met. **23**, 1 (1988).
[11]S. A. Safran, Phys. Rev. Lett. **44**, 937 (1980).
[12]S. E. Millman and G. Kirczenow, Phys. Rev. B **28**, 3482 (1983).
[13]N. Kambe, M. S. Dresselhaus, G. Dresselhaus, S. Basu, A. R. McGhie, and J. E. Fischer, Mater. Sci. Eng. **40**, 1 (1979).
[14]D. Billaud, E. McRae, J. F. Mareche, and A. Herlod, Synth. Met. **3**, 21 (1981).
[15]J. E. Fischer and H. J. Kim, Synth. Met. **23**, 121 (1988).
[16]D. Guerard and A. Herold, Carbon **13**, 337 (1975).
[17]Charles L. Mantell, *Carbon and Graphite Handbook* (Interscience, New York, 1968).
[18]W. Ruland, Acta Crystallogr. **18**, 992 (1965).
[19]R. Greissen, Phys. Rev. B **27**, 7575 (1983).
[20]P. M. Richards, Phys. Rev. B **30**, 5183 (1984).
[21]W. R. McKinnon and R. R. Haering, in *Modern Aspects of Electrochemistry,* edited by R. E. White, J. O'M Bockris, and B. E. Conway (Plenum, New York, 1983), No. 15, p. 235.
[22]A. N. Dey and B. P. Sullivan, J. Electrochem. Soc. **117**, 222 (1970).
[23]Y. Takada, R. Fujii, and K. Matsuo, Tanso **114**, 120 (1983).
[24]M. Arakawa and J. Yamaki, J. Electroanal. Chem. **219**, 273 (1987).
[25]R. Fong, U. von Sacken, and J. R. Dahn, J. Electrochem. Soc. **137**, 2009 (1990).
[26]R. G. Wyckoff, *Crystal Structures,* 2nd ed. (Krieger, Malabar, Florida, 1982), Vol. 1.
[27]J. R. Dahn, M. A. Py, and R. R. Haering, Can. J. Phys. **60**, 307 (1982).
[28]J. R. Dahn and D. P. Wilkinson (unpublished).
[29]J. R. Dahn and W. R. McKinnon, Solid State Ionics **23**, 1 (1987).
[30]J. R. Dahn, W. R. McKinnon, and S. T. Coleman, Phys. Rev. B **31**, 484 (1985).
[31]S. Lee, H. Miyazaki, S. D. Mahanti, and S. A. Solin, Phys. Rev. Lett. **62**, 3066 (1989).
[32]J. R. Dahn, D. C. Dahn, and R. R. Haering, Solid State Commun. **42**, 179 (1982).
[33]K. Huang, *Statistical Mechanics* (Wiley, New York, 1963).